Unravelling Irreversible Adsorbate Thermodynamics through Adsorption Assisted Desorption

Journal:	*Langmuir*
Manuscript ID	la-2023-03095b.R2
Manuscript Type:	Article
Date Submitted by the Author:	n/a
Complete List of Authors:	Lawal, Ajibola; University of Massachusetts Amherst, Chemical Engineering Abdelrahman, Omar; University of Massachusetts Amherst, Chemical Engineering

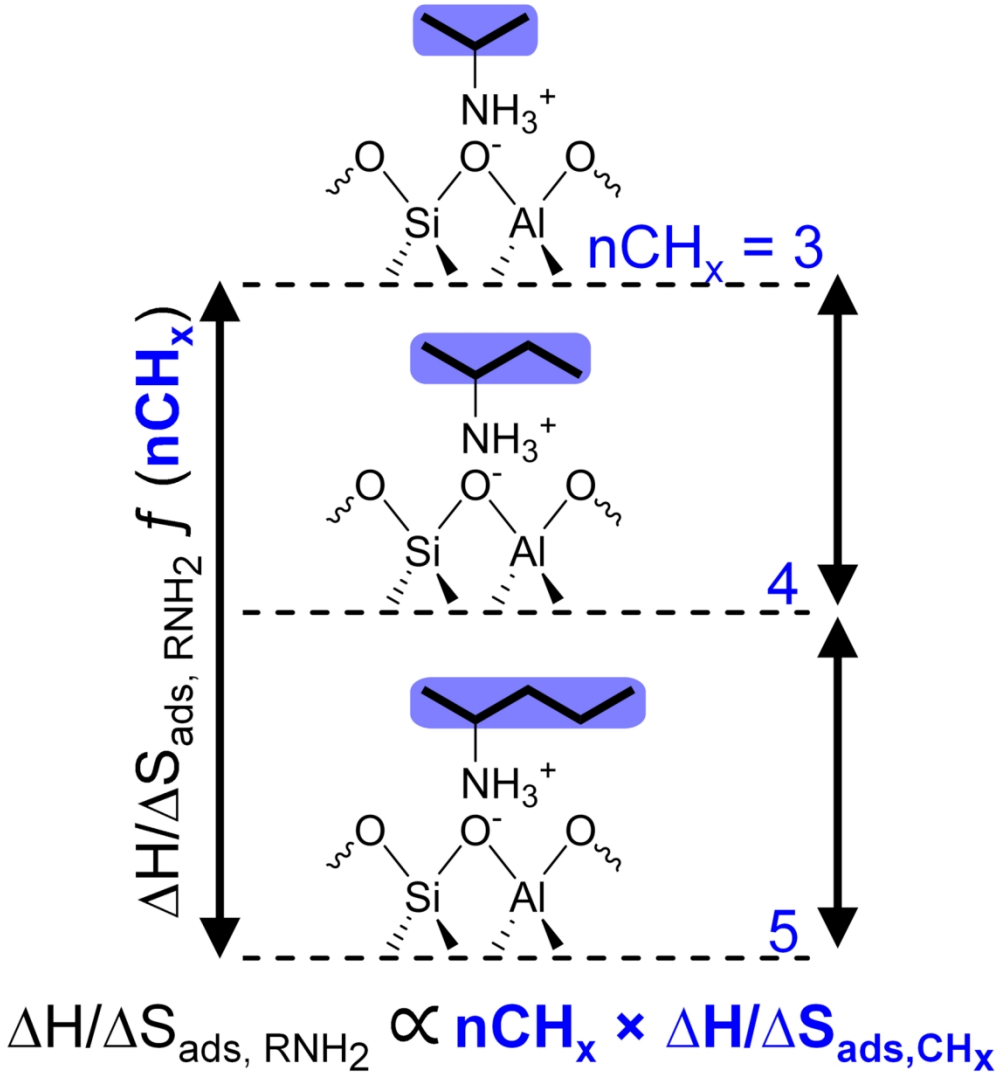

TOC

75x82mm (600 x 600 DPI)

Unravelling Irreversible Adsorbate Thermodynamics through Adsorption-Assisted Desorption

Ajibola Lawal and Omar A. Abdelrahman*

Department of Chemical Engineering, University of Massachusetts Amherst, 686 N. Pleasant Street, Amherst, MA 01003.

*Corresponding Author: abdel@umass.edu

Keywords: Entropy, Zeolites, Alkylammonium, Ion pair Adsorbates, Irreversible Adsorption, Chemisorption, Adsorption-assisted desorption

Abstract. Strongly bound surface species like alkylamines adsorbed on the Brønsted acid site of aluminosilicate zeolites exhibit negligible rates of molecular desorption, preventing them from achieving an equilibrated state on experimentally relevant timescales that limit the measurement of their adsorption thermodynamics. Through adsorption-assisted desorption, whereby distinct alkylamines facilitate desorption from Brønsted acid sites, we demonstrate that equilibrated states are achieved. Breakthrough adsorption measurements reveal that while 2-butylammonium on a Brønsted acid site is irreversibly adsorbed, it readily undergoes molecular desorption when exposed to a distinct alkylamine like 2-propanamine. As a result, two-adsorbate equilibrium was achieved when exposing Brønsted acid sites of aluminosilicate zeolites to a binary vapor phase alkylamine mixture. By varying relative vapor phase partial pressures and temperatures, we demonstrate the ability to experimentally measure the adsorption enthalpy and entropy of alkylammonium adsorbates on mostly isolated Brønsted acid sites in H-ZSM-5 (Si/Al = 140). A multi-adsorbate Langmuir isotherm was found to quantitatively describe the co-adsorption of alkylamines varying in size and basicity over a wide range of conditions, through which the relative adsorption enthalpy and entropy of alkylamines were measured. Across a homologous family of sec-alkylamines (C_3-C_5) adsorbed on isolated Brønsted acid sites, a fixed contribution to the enthalpy (19 ± 4 kJ mol CH_2^{-1}) and entropy (25 ± 4 J mol CH_2^{-1} K^{-1}) of adsorption per methylene unit of was found to exist, likely resulting from electrostatic interactions between the alkyl chain and surrounding pore environment.

Introduction. Alkylamines have long served as powerful probe molecules for the characterization and design of porous materials,[1, 2] proving especially useful for characterizing the density,[3, 4] identity,[5] location,[6, 7] and spatial proximity[8] of acid sites in heteroatom substituted zeolites. Upon adsorption, alkylamines additionally influence the catalytic activity and selectivity of zeolites, through post-synthetic modification of the active site environment in zeolite pores.[9, 10] Underpinning the utility of alkylamines on zeolite surfaces is the formation of a chemisorbed alkylammonium ion upon adsorption onto a Brønsted acidic site,[11] the stability of which is governed by both adsorbate enthalpy and entropy, with the role of entropy underscored at higher temperatures.[12] Through a combination of calorimetry based measurements and conceptual Born-Haber cycles, the adsorption enthalpy of alkylamines on Brønsted acid sites has been shown to linearly scale with their gas phase proton affinity.[13-16] The corresponding entropy of adsorption for alkylamines, however, has remained relatively unexamined. Prior work by Campbell and Sellers

developed a correlation predicting that adsorbates retain approximately two thirds of their gas phase entropies on single crystal surfaces,[17] which was later extended by Abdelrahman and Dauenhauer to account for pore confinement in zeotype materials.[18] However, such correlations are entirely based on molecules reversibly adsorbed to a surface (e.g. alkane adsorption), and are not applicable to adsorbates like alkylamines that are irreversibly adsorbed on Brønsted acid sites. To better leverage alkylamine probe molecule interactions in zeolites, experimental measurements of the entropy of these chemisorbed species are needed.

Entropy details the extent of an adsorbate's movement on a surface, describing its mobility through fundamental motions like translation, rotation, and vibration.[18] Adsorbate entropy has been determined via temperature programmed desorption on single crystal surfaces, however, re-adsorption events in porous materials[19, 20] limit its use for zeolites. Over porous materials like zeolites, experimental measurements of adsorbate entropy typically rely on equilibrium adsorption isotherms, where adsorbing molecules are in equilibrium with their bulk phase counterparts.[21, 22] The need for equilibrium poses a challenge for measuring the adsorption thermodynamics of chemisorbed moieties: desorption is significantly slower than adsorption and prevents adsorption-desorption equilibrium from being achieved at experimentally relevant timescales.[23, 24] The relatively slow rate of desorption is due to the large thermal barrier (e.g. 200 kJ mol^{-1} for pyridine on H-ZSM-5)[25] for desorption of a species chemisorbed on a surface. While elevated temperatures accelerate the rate of desorption, adsorbates like alkylamines on a zeolite surface become chemically reactive at temperatures necessary for feasible desorption rates.[26] As a result, entropy measurements of chemisorbed moieties on a surface through existing methods are exceedingly challenging and rare. Accelerating the rate of desorption, such that an equilibrium adsorption state can be achieved, is therefore necessary to measure the entropy of molecules that undergo chemisorption.

One approach to accelerate the rate of desorption is adsorption-assisted desorption, where the adsorption of one molecule, facilitates the desorption of another already adsorbed on the surface.[27] The concept was originally demonstrated on polycrystalline palladium, where the rate of CO^{18} desorption from the metal surface was accelerated in the presence of gaseous CO^{16}.[28]Similar isotopic approaches demonstrated the adsorption-assisted desorption of ammonia on the surface of γ-alumina, which otherwise remained irreversibly adsorbed below 473 K.[29] Adsorption-assisted desorption was also found to hold for chemically distinct adsorbates. For example, Lercher et al. observed that while methylamine on the Brønsted acid sites of Mordenite zeolites was chemisorbed as a methylammonium ion, it was readily displaced by ammonia through adsorption-assisted-desorption.[30] Similarly, Bell and co-workers noted a sharp increase in the rate of isobutene amination over the Brønsted acid sites of H-ZSM-5 upon the introduction of a pulse of n-propylamine, which facilitated the desorption of the otherwise chemisorbed t-butylamine product.[31] Given that the rate of adsorption remains unchanged, the effective rate of desorption is accelerated through adsorption-assisted desorption.

Recognizing its ability to preferentially accelerate the rate of desorption, we propose that adsorption-assisted desorption can be leveraged to equilibrate the adsorption of chemisorbed species on a surface. To this end, we investigated the adsorption thermodynamics of primary alkylamines on the Brønsted acid sites of H-ZSM-5, by simultaneously exposing the surface of H-ZSM-5 to distinct alkylamines that participate in adsorption-assisted desorption. While alkylamines irreversibly adsorb individually, binary mixtures of alkylamines established an equilibrium dictated coverage on available Brønsted acid sites, measured via their selective and chemically distinct Hofmann elimination[4] (**Scheme 1**). Alkylamine coverages were governed by

relative free energies of adsorption, and by extension, their relative enthalpies and entropies of adsorption. By controlling the zeolite Al content (Si/Al = 140) to expose mostly isolated Brønsted acid sites,[32, 33] differences in the entropy and enthalpy of isolated alkylammonium adsorbates in the pore of H-ZSM-5 were measured, where a fixed contribution to surface enthalpy and entropy per methylene unit was observed for C3-C5 sec-alkylamines.

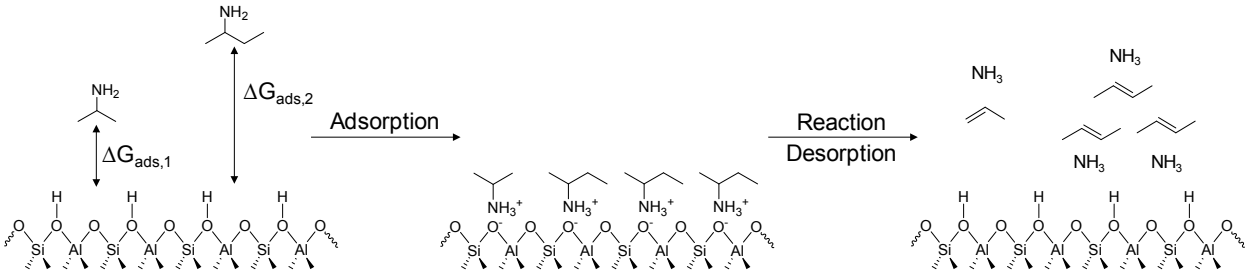

Scheme 1. Competitive adsorption between 2-propanamine and 2-butanamine over Brønsted acid sites, where relative coverages at equilibrium are dictated by relative free energies of adsorption. Coverages of the different alkylamines on the surface can be directly measured by quantifying their respective Hofmann elimination alkene product.

Experimental

Materials. 2-propanamine (99.5%, Sigma Aldrich), 2-butanamine (99%, Sigma Aldrich), 2-pentanamine (97%, Sigma Aldrich), n-heptane (99%, Sigma Aldrich), type 1 water (> 18.2 MΩ-cm) obtained from an in-house purifier (Spectrapure), were used as adsorbates and/or for instrument calibration. He (99.999%, Airgas), Ar (99.999%, Airgas), N_2 (99.999%, Airgas), Air (Ultra-zero, Airgas) were used as carrier gas and for zeolite pretreatment.

Zeolite Pre-treatment. Ammonium-form ZSM-5 was obtained from Zeolyst International (CBV28014, Si/Al=140) and converted to its hydrogen form by ex-situ calcination in a stream of air (100 sccm) at 823 K using a ramp rate of 2 K min^{-1} for 10 hours. The calcination was performed in a downward flow quartz u-tube, where the flow of air was controlled by a mass flow controller (Brooks 5850). The zeolite temperature was monitored using a 1/16" type K thermocouple (KQXL-116G-12, Omega) encased in a 3 mm quartz sheath (2x3, Technical Glass Products), placed in contact with the zeolite bed. Details of the setup are provided in the supporting information (**Sec. S1**). To ensure a clean surface prior to adsorption, the zeolite bed was also calcined in-situ at 673 K with a ramp rate of 10 K min^{-1} and 100 sccm of air.

Zeolite Pelletization. To control the particle size of the zeolite, it was pelletized, broken, and sieved into different fractions. Typically, 100 mg of ex-situ calcined zeolite was placed between two mirror polished dice of a pellet press (13 mm diameter, 161-1900, Pike Technologies) and pressed to a pressure of ~20 MPa sufficient to form pellet without structural changes,[37] using a vertical hydraulic jack (YLJ-5-H, MTI Corporation). The pelletized zeolite was carefully broken into small pieces using an Agate mortar and pestle (89037-488, VWR), and sieved into different pellet diameters using 3-inch sieves (EW-59987-09, EW-59987-14, EW-59987-19, EW-59987-24, EW-59987-28, and EW-59988-03, Cole Parmer) by shaking intermittently for 3-5 minutes.

Inlet Liner Microcatalytic Reactor. We have previously demonstrated the use of gas chromatography (GC) inlet liners as microcatalytic reactors[4] and employ the same procedure here.

Briefly, a pelletized zeolite bed was placed between two plugs of deactivated quartz wool (Restek, 24324), packed into a commercially available quartz GC inlet liner (Agilent 5190-3165). The quartz wool served as an inert physical support as well as a dispersant to efficiently vaporize injected liquid adsorbates, prior to contacting the zeolite. To ensure accurate temperature control and a negligible axial temperature distribution (< 1 K), the zeolite bed was always located between 20 and 40 mm from the bottom of the liner.[38] Unless otherwise noted, zeolite pellet diameter was controlled between 500 – 1000 μm. Typically, ~20 mg of pelletized zeolite was loaded into the inlet liner microcatalytic reactor; the mass of the entire microreactor packed with quartz wool was measured before and after adding the zeolite to ensure accurate loadings.

Fractional Coverage. Reactive gas chromatography was used to measure the fractional coverage of alkylamines (θ_i) occupying Brønsted acid sites (**Fig. 1**). We have previously reported details of this method elsewhere for single adsorbates, used to estimate the Brønsted acid site density of aluminosilicate zeolites.[4] Briefly, the zeolite containing quartz liner was placed in the inlet of a gas chromatograph (7890B, Agilent), where it was first calcined in-situ at 673 K, then cooled down in He to the temperature at which fractional coverages are measured (**Fig. 1A,D,G**). Using an automated liquid sampler, a mixture of alkylamines was injected at 1 μL min^{-1} into a 1000 sccm He carrier stream, creating a binary alkylamine vapor mixture with defined partial pressures (**Fig. 1 B,E,G**). The molar composition of the pre-made liquid alkylamine mixture was independently confirmed on a separate gas chromatograph equipped with an HP-5 column (19091J-413, Agilent) and flame ionization detector (FID), coupled with a quantitative carbon detector (Polyarc, Activated Research Company).[39] The zeolite was then exposed to the binary alkylamine vapor mixture until saturation (typically 15 μL total dose volume), after which the zeolite bed was purged for two hours in He (1000 sccm) to remove any physisorbed species. Prior to raising the temperature of the zeolite bed, the temperature of the gas chromatograph oven containing the chromatographic column (19091-Q04, Agilent) was lowered to 303 K. Directing the microcatalytic reactor effluent through the chromatographic column at a low temperature, along with a suitable choice of column stationary phase, trapped desorbing molecules from the zeolite surface. The temperature of the microcatalytic reactor was then ramped at a rate of 10 K min^{-1} to 673 K and held for 30 minutes, allowing for adsorbed alkylamines to either desorb intact or undergo a Hofmann elimination to their respective products (alkene + NH_3). The temperature of the column, containing the trapped molecules, was then raised from 303 to 543 K at a ramp rate of 10 K min^{-1} and held there for 10 minutes. Alkene peaks corresponding to the respective alkylamines were detected. Based on our prior measurements, the Brønsted acid site density of H-ZSM-5 (Si/Al = 140) is taken to be 100 μmol H^+ g^{-1} (n_{BAS}),[4] with a 6% fraction of framework incorporated Al that are next-nearest neighbors (paired).[8] Use of a high Si/Al ratio yields an H-ZSM-5 with mostly isolated Brønsted acid sites, where the opportunity to investigate the adsorption energetics of relatively isolated adsorbates was afforded. Regardless of the alkylamine combination co-adsorbed, the total Brønsted acid site density measured was found to remain unchanged ($\sum_i n_{Alkene,i} = n_{BAS}$), and the coverage of vacant sites to be zero ($\theta_* = 0$, supporting information, **Sec. S3**). The strong interaction of alkylamines with Brønsted acid sites results in a completely saturated surface even at relatively limited alkylamine partial pressures,[4] which was further validated through FTIR measurements (**Supporting Information, Sec. S9**). The total moles of alkene evolved ($\sum n_{alkene,i}$) was therefore taken to be equal to the number of Brønsted acid sites (n_{BAS}) occupied by the corresponding alkylamine, allowing the fractional coverage of a particular alkylamine to be estimated,

$$\theta_i = \frac{n_{Alkene,i}}{n_{BAS}} = \frac{n_{Alkene,i}}{\sum_i n_{Alkene,i}} \quad (1)$$

For example, with 2-propanamine and 2-butanamine (**Scheme 1**), the fractional coverage of 2-propanamine equals the moles of propene evolved divided by the total moles of propene and butene(s) evolved. The average error in coverages was found to be less than 10% based on repeated measurements.

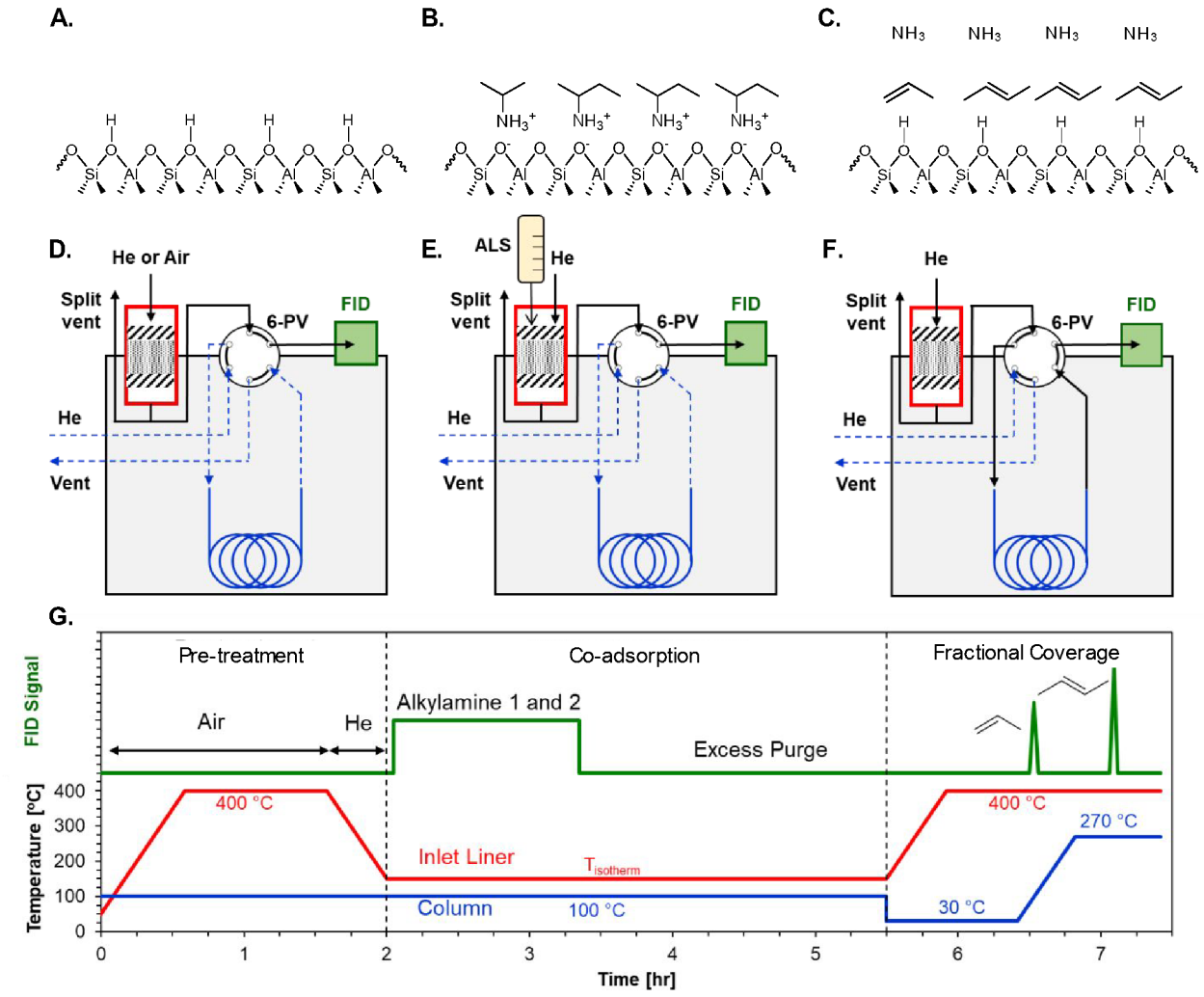

Figure 1. Reactive Gas Chromatography (RGC) to measure co-adsorbed alkylamine coverage A. Aluminosilicate Brønsted acid sites **B.** 2-propanamine and 2-butanamine adsorption on Brønsted acid sites, fractional coverages are determined by relative adsorption energetics and partial pressures **C.** Reactive desorption via Hofmann elimination, forming propene, butene(s) and ammonia **D. Pre-treatment:** Zeolite calcined in-situ at 673 K, cooled to co-adsorption temperature under helium atmosphere **E. Co-adsorption:** An automatic liquid sampler (ALS) injects a pre-determined mixture of alkylamines into a helium flow, creating a relative alkylamine partial pressure ($P_{Alkylamine,1}/P_{Alkylamine,2}$) that co-adsorbs on the zeolite surface, then purged to remove

physisorbed amines **F. Fractional Coverage:** Linear temperature ramp of zeolite to 673 K while desorbing alkenes are trapped in chromatography column held at 303 K. The column temperature is linearly ramped to elute trapped alkenes corresponding to alkylamines adsorbed on Brønsted acid sites, independently quantified via a flame ionization detector (FID) **G. Temporal profile:** Zeolite containing quartz liner temperature, chromatography column temperature, and corresponding FID signal as a function of time during pre-treatment, alkylamine co-adsorption, and fractional coverage estimation.

Breakthrough Adsorption-Assisted Desorption. About 50 mg of zeolite was placed in a 1/2″ quartz downflow packed bed u-tube, with the zeolite bed resting on a plug of deactivated quartz wool. The packed bed was placed within a ceramic furnace (VF-360-1.5-6-S, Thermcraft) controlled using a PID temperature controller (CN 7823, Omega) and a 1/16″ type K thermocouple (KQXL-116G-12, Omega) encased in a 12 mm quartz sheath (2x3, Technical Glass Products), placed on top of the bed. The entire heated assembly was housed within a larger forced convection oven (5890 Series II, Hewlett Packard) held at 373 K. Gas flows were controlled by a mass flow controller (5850S, Brooks Instrument). The zeolite was calcined in-situ under 60 sccm of air at 823 K for 4 hours with a ramp rate of 5 K min^{-1} and then cooled to 423 K, before purging in 100 sccm of He for 15 minutes. Liquid-phase alkylamines were fed to distinct vaporization sections through a 1/16″ PEEK capillary line (0.01″ I.D., TPK110, Vici Valco) using a syringe pump (Masterflex EW-74905-04, ColeParmer) and air-tight glass syringes (81220 and 81420, Hamilton Company), the vaporized alkylamines were either vented or plumbed to a static mixer as determined by a four-port switching valve (A24UWE, Vici Valco). The PEEK line was connected to a 1/16″ stainless-steel capillary line (0.01″ I.D., T50C10D, Vici Valco) through a PEEK union (ZU1FPK, Vici Valco), with the other end of the stainless-steel capillary line was placed inside the oven. The vaporized alkylamine was constantly swept by a 100 sccm stream of He, which bypassed or adsorbed onto the zeolite bed as determined by a six-port switching valve (A26UWE, Vici Valco). 2-butanamine (C_4) was introduced as the initial adsorbate at 0.3 kPa in He (100 sccm) at 423 K for 30 minutes, where protonated 2-butylammonium formed on the zeolite surface, followed by a 2 hour purge in He to remove any physisorbed 2-butanamine. The second adsorbate, 2-propanamine (C_3) was then introduced into a He stream, in a different vaporization section using the four-port switching valve (A24UWE, Vici Valco), bypassing the zeolite containing packed bed at a partial pressure of 0.3 kPa. The bypass stream was analyzed with an online residual gas analyzer (XT200M, ExTorr) with C_3 at a mass to charge ratio (m/z) of 44. After ~30 minutes, the C_3 containing He stream was sent through the zeolite bed using a six-port switching valve (A26UWE, Vici Valco), exposing the 2-butylammonium containing zeolite bed to 2-propanamine. Desorption of the initially adsorbed C_4, assisted by the adsorption of the C_3, was observed by tracking the mass-to-charge (m/z) ratios of 44 and 55 associated with C_3 and C_4, respectively (supporting information, **Sec. S4**).

Results & Discussion. Alkylamines interact strongly with the Brønsted acid sites (BAS) of aluminosilicate zeolites, resulting in a complete transfer of the Brønsted acidic proton of the bridging hydroxyl (ZOH) to the alkylamine, forming an alkylammonium ion (RNH_3^+),[3, 40]

$$RNH_2 + ZOH \rightleftharpoons ZO^- RNH_3^+ \quad (2)$$

where ZO^- represents the deprotonated state of the BAS. Alkylamine adsorption on a Brønsted acidic proton is typically accompanied by a relatively large enthalpy change; 2-propanamine adsorbs on H-ZSM-5 with an adsorption enthalpy (ΔH_{ads}) of ~ 200 kJ mol^{-1}.[34] As a result, alkylamines and other related molecules like pyridine are frequently used as BAS poisons, adsorbing strongly enough to displace most other adsorbates (e.g. alcohols,[4, 41] alkanes,[42, 43] alkenes[44]). Therefore, alkylamine adsorption is commonly treated as irreversible at moderate temperatures (T < 600 K).[25] Here, we hypothesize that despite the highly favorable adsorption of alkylamines on BAS, two distinct alkylamines can sufficiently compete for adsorption on the same BAS, resulting in constant alkylamine adsorption/desorption until an equilibrated state is reached. To our knowledge, the molecular desorption of a primary alkylamine intact from an aluminosilicate BAS, or displacement by another adsorbate has not been demonstrated. It is therefore necessary to confirm whether two distinct alkylamines (e.g. 2-propanamine and 2-butanamine) can displace one another from a BAS.

Alkylamine Adsorption-Assisted Desorption. While the exact mechanism by which the exchange of alkylamines could proceed is unclear, we propose a potential mechanism based on the concept of adsorption-assisted desorption.[27, 30] In the case where C_4 is initially adsorbed, it first adsorbs and abstracts a proton from the Brønsted acid site to from a 2-butylammonium ion (C_4^+). When a second adsorbate like 2-propanamine is subsequently introduced, it abstracts a proton from C_4^+ and forms 2-propylammonium (C_3^+). The overall process can be described through three elementary steps:

$$C_4 + ZOH \rightleftharpoons ZO^-C_4^+ \quad (3)$$

$$C_3 + ZOH \rightleftharpoons ZO^-C_3^+ \quad (4)$$

$$C_3 + ZO^-C_4^+ \rightleftharpoons C_4 + ZO^-C_3^+ \quad (5)$$

Eq. 3 and 4 represent the thermodynamic information associated with each independent alkylamine's adsorption. We propose that transfer of the proton from one alkylamine to another (Eq. 5) occurs in a concerted fashion, potentially passing through an activated transition state (**Scheme 2A**). Ultimately, 2-propanamine facilitates the displacement of 2-butanamine from the Brønsted acid site through adsorption-assisted desorption. As a result, adsorption-assisted desorption over a BAS will be dictated by the relative adsorption enthalpy ($\Delta\Delta H_{ads}^0$, **Scheme 2B**) and entropy ($\Delta\Delta S_{ads}^0$, **Scheme 2C**) of the two distinct alkylamines.

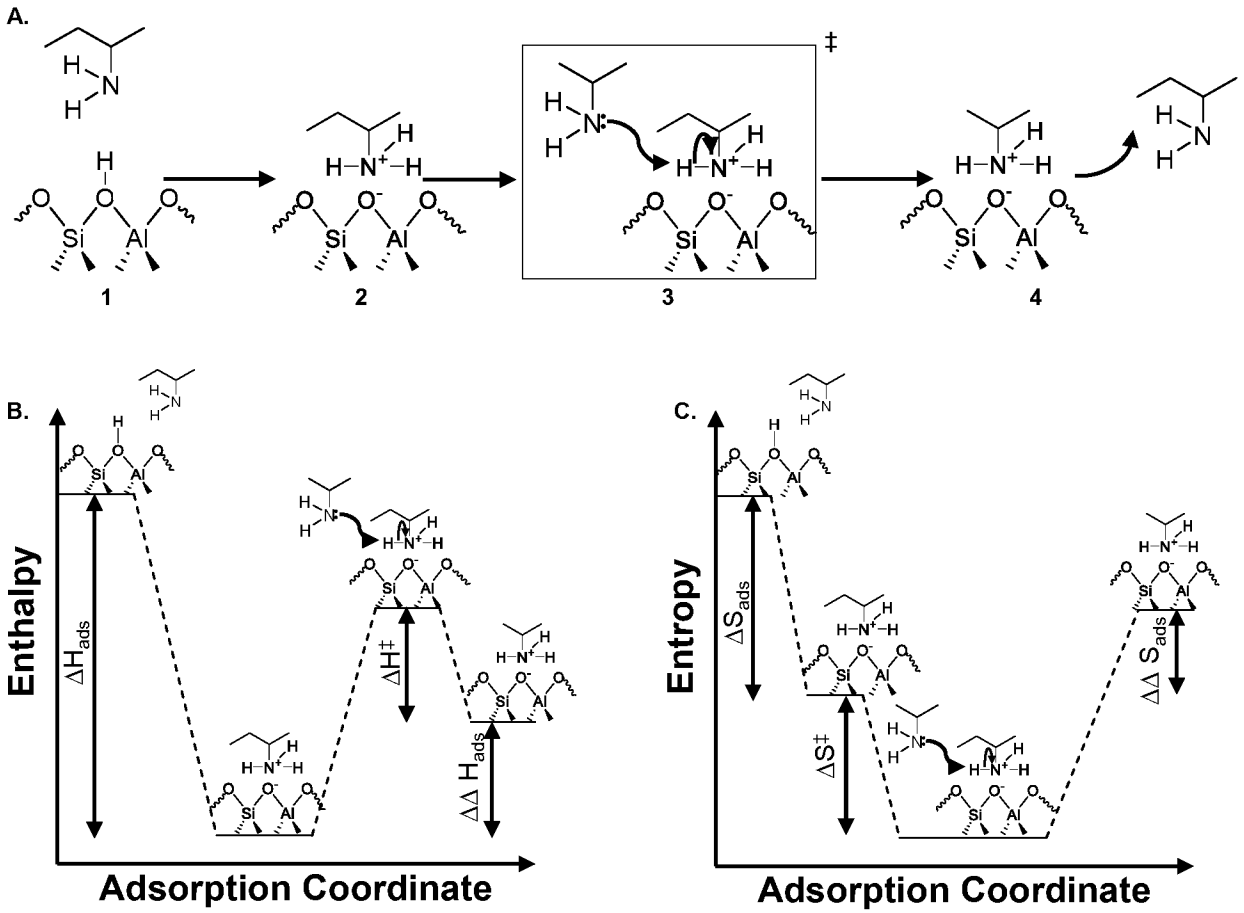

Scheme 2. Alkylamine Adsorption-Assisted Desorption over an Aluminosilicate Brønsted Acid Site A. Adsorption of 2-butanamine onto an aluminosilicate Brønsted acid site, followed by a proton abstraction and its subsequent desorption by 2-propanamine **B.** Adsorption enthalpy of 2-propanamine and the relative adsorption enthalpy of 2-butanamine as it is displaced by 2-propanamine from the surface through an activated complex of both amines **C.** Adsorption entropy of 2-propanamine and the relative adsorption entropy of 2-butanamine as it is displaced by 2-propanamine from the surface, while forming an activated complex of both amines.

To investigate the possibility of alkylamine adsorption-assisted desorption, a breakthrough analysis of alkylamine-adsorption was leveraged. H-ZSM-5 with complete coverage of 2-butanamine (adsorbed as 2-butylammonium), was exposed through an instantaneous switch to a 2-propanamine containing helium stream in a continuous flow packed bed (**Fig. 2**). H-ZSM-5 was first saturated with a vapor phase stream of 2-butanamine at 423 K, resulting in a surface completely covered by 2-butylammonium moieties at all anionic bridging oxygen locations in the zeolite framework (Eq. 3). Once exposed to 2-propanamine, 2-butanamine was observed to desorb from the surface, replaced by 2-propanamine over the Brønsted acid sites (adsorbed as 2-propylammonium, **Fig. 2**). Increasing the temperature of the 2-butylammonium covered H-ZSM-5 to 498 K prior to 2-propanamine exposure led to similar observations of adsorption-assisted desorption (supporting information, **Sec. S5**), suggesting minimal contribution by physisorbed alkylamines.

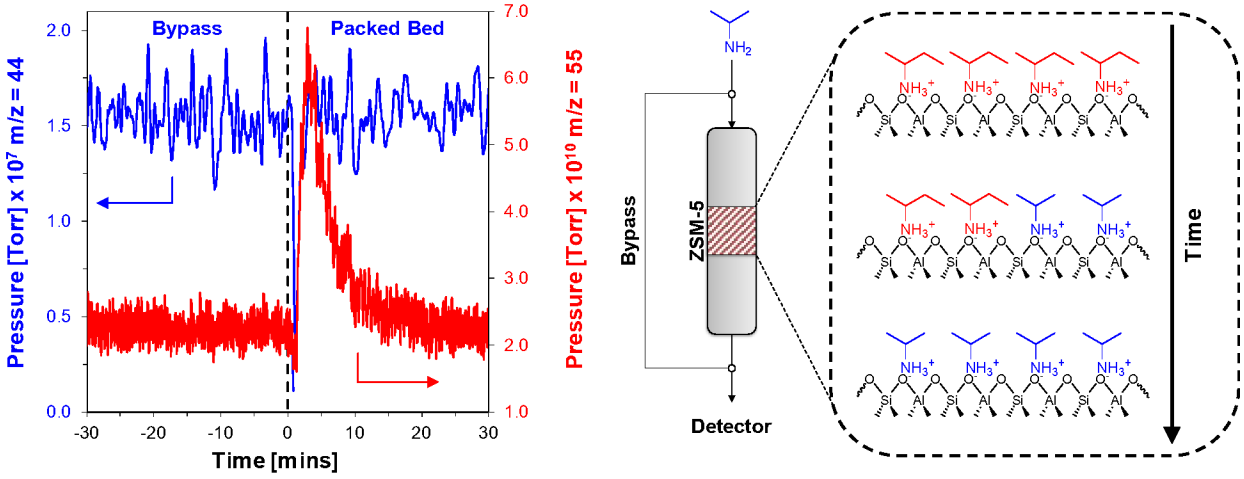

Figure 2. 2-propanamine-Assisted Desorption of 2-butanamine on H-ZSM-5. Breakthrough of 2-propanamine adsorption-assisted desorption over a 2-butylammonium saturated H-ZSM-5 at 423 K. Effluent 2-propanamine and 2-butanamine were tracked through mass to charge ratios (m/z) of 44 and 55, respectively.

To verify that an initially adsorbed alkylamine was in fact displaced by a second adsorbing alkylamine, forming a distinct alkylammonium adsorbate, alkylammonium surface coverages in the course of adsorption-assisted desorption were quantitatively measured. Similar to the breakthrough analysis, H-ZSM-5 was first saturated with an alkylamine (initial adsorbate) and purged to remove any physisorbed species, followed by exposure to another distinct alkylamine (second adsorbate). Initial and second alkylamine adsorbates with distinct Hofmann elimination alkene products were selected, such that their respective coverages could be readily determined. Consistent with the observed displacement based on measured vapor phase partial pressures (**Fig. 2**), the surface of H-ZSM-5 initially saturated with 2-butylammonium, exhibited complete coverage of 2-propylammonium after exposure to 2-propanamine. The reverse was also found to be true; 2-butanamine as a second adsorbate quantitatively displaced 2-propylammonium from the surface of H-ZSM-5. Regardless of alkylamine combination and sequence, distinct alkylamines were able to displace one another from a BAS (**Table 1**), suggesting that when multiple alkylamines are concurrently present, they continuously displace each other until an equilibrium coverage is attained. As a control, we examined second adsorbates more-weakly bound than alkylamines; both n-heptane and water were incapable of displacing 2-butanamine adsorbed on a Brønsted acid site (**Table 1**). The inability to displace 2-butanamine is not surprising given the large difference in proton affinity between n-heptane (680 kJ mol^{-1})[45] or water (691 kJ mol^{-1}) and 2-butanamine (930 kJ mol^{-1}).[46] Similarly, Gorte et. al reported that n-hexane could not displace pyridine adsorbed on a BAS within H-ZSM-5, while the reverse was shown to be possible.[47]

Table 1. Fractional coverages of alkylamines on H-ZSM-5 as exposed to initial and second adsorbates.

Initial Adsorbate	Second Adsorbate	$\theta_{Initial}$	θ_{Second}
C_4	C_3	0.94	0.06
C_3	C_4	0.99	0.01
C_5	C_3	0.73	0.16
C_3	C_5	0.99	0.01
C_5	C_4	0.93	0.07

C_4	C_5	0.97	0.03
C_4	n-heptane	1.00	n.m.
C_4	H_2O	1.00	n.m.

C_3; 2-propanamine, C_4; 2-butanamine, C_5; 2-pentanamine.
He carrier stream flow rate = 100 sccm
T = 423 K

Alkylamine Competitive Adsorption. Having established alkylamine adsorption-assisted desorption, through sequential exposure, the competitive adsorption of gas phase alkylamine mixtures on Brønsted acid sites in H-ZSM-5 was examined. Measuring the fractional coverages of two distinct adsorbing alkylamines provides a measure of their relative adsorption energetics (**Scheme 2**). It is therefore necessary to ensure that measured fractional coverages are not influenced by non-thermodynamic contributions. Given the relative dimensions of the pores of ZSM-5 and alkylamine molecular diameters, the potential influence of mass transfer was examined. Changes in total pressure, while fixing relative alkylamine partial pressure, lead to no measurable change in the distribution of alkylamine fractional coverage (**Fig. 3A**); alkylamine coverages on the surface are only dictated by vapor phase mole fractions. Similarly, the average H-ZSM-5 pellet diameter was inconsequential to the measured fractional coverage (**Fig. 3B**). Conversely, the flow rate of the vapor phase from which alkylamines adsorbed on H-ZSM-5 was found to influence measured fractional coverages; increasing the flow rate from 10 - 1000 sccm led to an increase in the fractional coverage of 2-propylammonium (**Fig. 3C**). An increased flow rate likely increased the rate of alkylamine diffusion to Brønsted acid sites from the bulk vapor phase, relative to the rate of adsorption-assisted desorption. Beyond a vapor phase flow rate of ~100 sccm, however, no measurable change in fractional coverage was observed. The flow rate of all subsequent fractional coverage measurements was therefore fixed at 1000 sccm.

Given that the kinetics of adsorption-assisted desorption relative to diffusion into the pore may play a significant role, we investigated the necessary extent of alkylamine exposure to ensure an equilibrated coverage. Here, we define the extent of exposure as the moles of amine exposed to the zeolite, normalized by the zeolite Al molar content,

$$\text{Extent of Exposure} = \frac{\dot{n}_{amine} * t_{exposure}}{n_{Al}} \left[= \right] \frac{\text{moles of alkylamine exposed}}{\text{moles of bulk Al in zeolite}} \quad (6)$$

where n_{amine}, $t_{exposure}$, and n_{Al}, are the amine molar flowrate, exposure time, and moles of Al present in the zeolite bed over which adsorption-assisted desorption takes place. As the exposure time increases, the moles of amine that the zeolite is exposed to increases, allowing for fractional coverages to equilibrate as dictated by relative adsorption energetics. Indeed, as the extent of 2-butanamine exposure increased, even beyond stoichiometric requirements, the fractional coverage of 2-butylammonium increased while that of 2-propylammonium decreased (**Fig. 3D**). The relative trend observed with increasing extent of 2-butanamine exposure is consistent with a slower rate of diffusion, relative to the smaller 2-propanamine. As a result, extents of exposure in excess of an order of magnitude were utilized to ensure fractional coverage measurements not influenced by mass transfer.

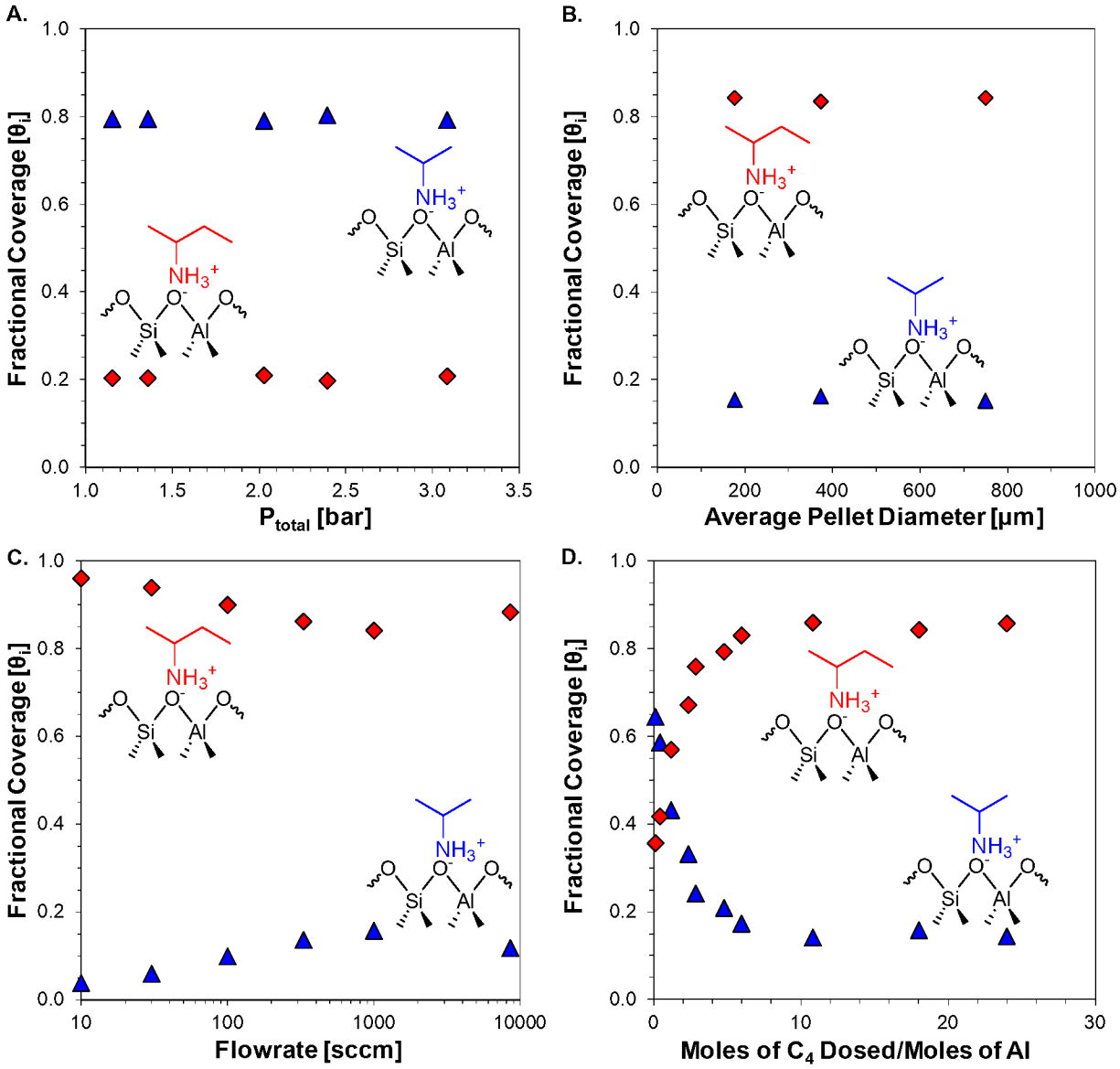

Figure 3. Fractional coverage of C_3 (▲), and C_4 (◆) on H-ZSM-5 at 423 K as a function of A. Total pressure, $P_{C3}/P_{C4} = 50$ **B.** Average zeolite pellet diameter, $P_{C3}/P_{C4} = 3$ **C.** He carrier gas flow rate, $P_{C3}/P_{C4} = 3$ **D.** Alkylamine extent of exposure (Eq. 6), $P_{C3}/P_{C4} = 3$.

Relative Energetics of Alkylamine Adsorption. Using the established parameters in the previous section, the competitive adsorption of 2-propanamine (C_3) and 2-butanamine (C_4) on H-ZSM-5 was carried out between 373 - 498 K, varying the relative partial pressure of adsorbates (P_{C3}/P_{C4}) from 0.5 – 50 (**Fig. 4**). Under the adsorption conditions considered, the Brønsted acid sites of H-ZSM-5 were completely covered by both adsorbates ($\theta_* = 0$, supporting information, **Sec. S3**). Here, we rationalize alkylamine fractional coverages through a dual-adsorbate Langmuir isotherm (supporting information, **Sec. S6**),

$$\theta_i = \frac{1}{1 + \frac{P_j}{P_i}\exp\left(\frac{\Delta G_{ads,i}^{0} - \Delta G_{ads,j}^{0}}{RT}\right)} \quad (7)$$

$$\Delta G^{ads,i0} - \Delta G^{ads,j0} = \Delta\Delta H^{ads,ij0} - T\Delta\Delta S^{ads,ij0} \quad (8)$$

where an alkylamine's fractional coverage (θ_i) is dictated by its vapor phase partial pressure (P_i) and adsorption free energy ($\Delta G_{ads,i}^{0}$). By comparing predicted ($\theta_{i,Predicted}$) and measured ($\theta_{i,Measured}$) fractional coverages, the relative adsorption enthalpy ($\Delta\Delta H_{ads,ij}^{0}$) and entropy ($\Delta\Delta S_{ads,ij}^{0}$) were fit through a least square regression (**Fig. 4A**). All confidence intervals for fitted values were reported at a 95% confidence level. Despite the similar nature of alkylamine adsorption,[3, 40] and proton affinities (924 and 930 kJ mol^{-1} for C_3 and C_4, respectively),[46] the additional methylene unit results in a significant adsorption energetic difference; 2-butanamine (C_4) loses more entropy than 2-propanamine (C_3) upon adsorption ($\Delta\Delta S_{ads}^{0}$ = 24 ± 7 J mol^{-1} K^{-1}) but is more enthalpically stabilized ($\Delta\Delta H_{ads}^{0}$ = 19 ± 3 kJ mol^{-1}). As a result, a relative partial pressure in excess of one order of magnitude ($P_{C3}/P_{C4} > 10$) is needed for C_3 to command a larger fractional coverage than C_4 on the Brønsted acid sites of H-ZSM-5 (498 K, **Fig. 4B**). Extending the length of the carbon chain over a similar range of experimental conditions (373-498 K, P_{C4}/P_{C5} = 0.5 - 46, **Fig. 4C,D**), 2-pentanamine loses more entropy than 2-butanamine upon adsorption ($\Delta\Delta S_{ads}^{0}$ = 25 ± 7 J mol^{-1} K^{-1}) but is more enthalpically stabilized ($\Delta\Delta H_{ads}^{0}$ = 18 ± 3 kJ mol^{-1}). A more favorable enthalpy of adsorption and the accompanying loss in entropy with increasing chain length, creating a compensation effect between the two thermodynamic quantities,[18] is consistent with prior reports of other hydrocarbon adsorbates in zeolites.[48, 49]

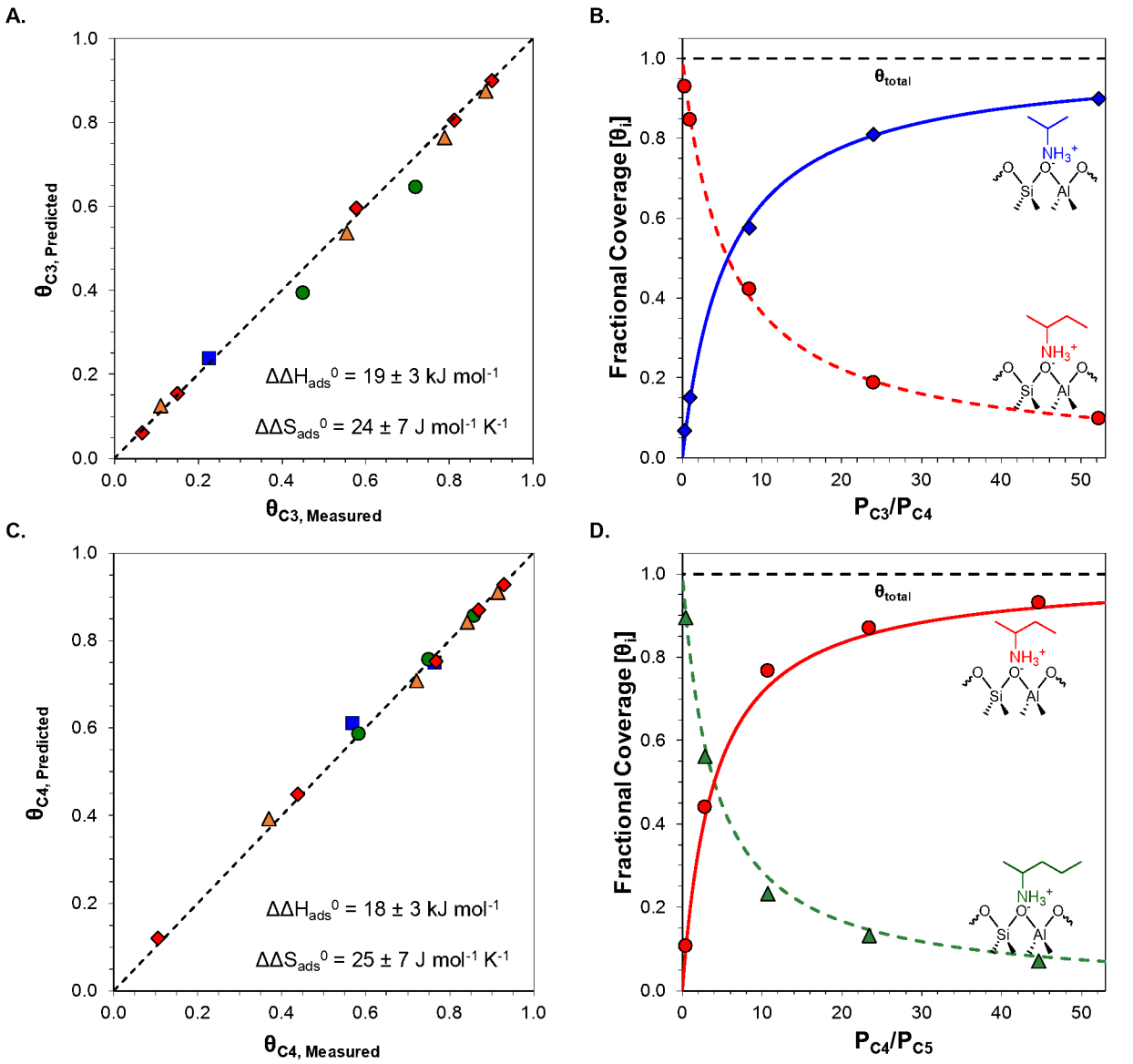

Figure 4. Alkylamine co-adsorption over H-ZSM-5 A. Parity plot comparing measured and predicted coverages of C_3 at 373 (■), 423 (●), 473 (▲) and 498 K (◆), based on a two-adsorbate competitive Langmuir adsorption isotherm for C_3 and C_4. **B.** Fractional coverages of C_3 (◆) and C_4 (●) as a function of their relative partial pressure at 498 K, θ_{total} indicates the total coverage **C.** Parity plot comparing measured and predicted coverages of C_4 at 373 (■), 423 (●), 473 (▲) and 498 K (◆), based on a two-adsorbate competitive Langmuir adsorption isotherm for C_4 and C_5 **D.** Fractional coverages of C_4 (●) and C_5 (▲) as a function of their relative partial pressure at 498 K, θ_{total} indicates the total coverage.

Predicted and Measured Adsorption Energetics. With the assumed thermodynamic nature of alkylamine adsorption-assisted desorption, the measured relative adsorption energetics are expected to behave as state functions,

$$\Delta\Delta H_{ads,ij}^{0} = \Delta\Delta H_{ads,ik}^{0} + \Delta\Delta H_{ads,kj}^{0} \quad (9)$$

$$\Delta\Delta S_{ads,ij}^{0} = \Delta\Delta S_{ads,ik}^{0} + \Delta\Delta S_{ads,kj}^{0} \quad (10)$$

where i, j, and k are three distinct adsorbing alkylamines. Here, we compared the relative adsorption energetics of C_3, C_4, and 2-pentanamine (C_5, **Fig. 5A**). Taking the sum of the measured relative adsorption enthalpies of C_3-C_4 (**1**) and C_4-C_5 (**2**), the predicted C_3-C_5 (**3**) relative adsorption enthalpy of 37 kJ mol^{-1} is in excellent agreement with an experimentally measured value of 36 kJ mol^{-1} (**Fig. 5B**). Similarly, the predicted and measured C_3-C_5 relative entropy of adsorption were found to be in excellent agreement (49 and 56 J mol^{-1} K^{-1}, respectively).

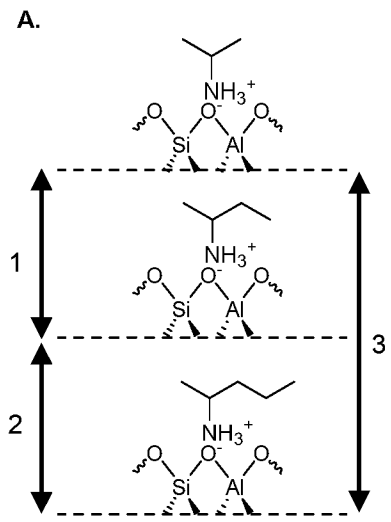

B.

			$\Delta\Delta H_{ads}$ [kJ mol^{-1}]	$\Delta\Delta S_{ads}$ [J mol^{-1} K^{-1}]
1	C_3-C_4	Measured	19 ± 3	24 ± 7
2	C_4-C_5	Measured	18 ± 3	25 ± 7
3	C_3-C_5	Predicted (1+2)	37	49
	C_3-C_5	Measured	36 ± 22	56 ± 29

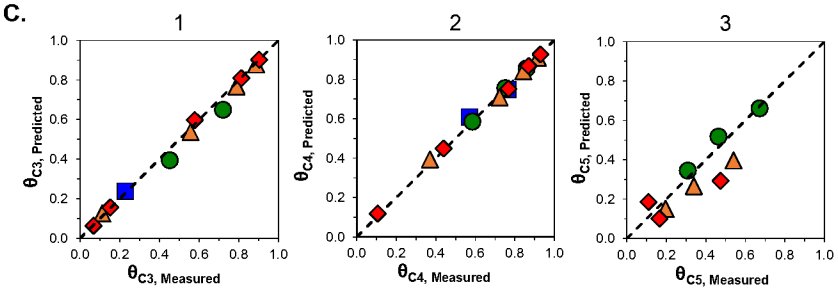

Figure 5. Relative adsorption energetics of C_3, C_4, and C_5 A. Relative energy levels of adsorbed 2-propylammonium (C_3), 2-butylammonium (C_4), and 2-pentylammonium (C_5). C_3-C_4 (1), C_4-C_5 (2), and C_3-C_5 (3) **B.** Comparison of measured and predicted C_3-C_5 relative adsorption enthalpy and entropy, per Eqs. 9-10 **C.** Parity plot comparing measured and predicted coverages at 373 (■), 423 (●), 473 (▲) and 498 K (◆) based on two-adsorbate competitive Langmuir adsorption isotherms of C_3-C_4 (1), C_4-C_5 (2), and C_3-C_5 (3).

Alkylamines and Alkanes. Comparing the relative adsorption energetics of the two distinct alkylamine pairs (C_3 /C_4 and C_4/C_5), a fixed contribution to the overall enthalpy and entropy of alkylamine adsorption per methylene unit is apparent. With each increasing methylene unit in the alkylamine carbon chain, an additional enthalpic stabilization of ~19 kJ mol CH_2^{-1} was experienced (**Fig. 6A**). Previous investigations on alkane adsorption in H-ZSM-5 reported an enthalpic stabilization of ~10 kJ mol CH_2^{-1},[49-54] attributed to lateral interactions between alkanes and the zeolite lattice oxygen. The change in alkane adsorption enthalpy was also accompanied by an entropic loss of ~10 J mol CH_2^{-1} K^{-1}, resulting from the additional confinement experienced by alkane adsorbates with increasing chain length (Supporting Information, **Sec. S8**).[49, 55] For the primary alkylamines in this work, each additional methylene unit lead to an additional 25 J mol CH_2^{-1} K^{-1} entropic penalty (**Fig. 6A**). Similar energetic trends therefore exist across the two homologous adsorbate families, albeit, with larger enthalpic and entropic contributions per methylene unit for alkylamines (**Fig. 6B**). One possible explanation for the larger enthalpic

stabilization per methylene unit in alkylamines is their larger proton affinity relative to alkanes (~ 900 vs ~ 600 kJ mol^{-1}), which can play a role even for the adsorption of weakly basic alkanes on aluminosilicate surfaces.[56] While alkanes adsorb on Brønsted acid sites through weaker interactions like hydrogen bonding,[52, 54] alkylamines abstract the proton to form alkylammonium ions on the zeolite surface (Eq. 2, **Fig. 6C**).[3, 40] Nevertheless, the similar trends in methylene contribution to adsorbate energetics suggest that Van der Waal interactions between adsorbates and the host zeolite environment are also likely responsible for changes in alkylamine adsorption energetics with chain length.

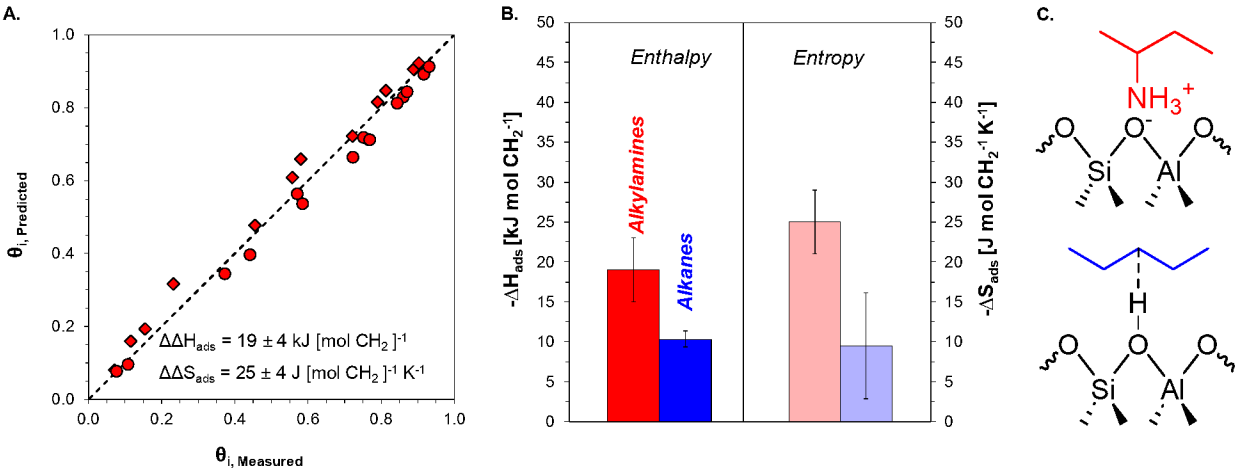

Figure 6. Adsorption Energetics per Methylene Unit of Alkanes and Alkylamines. A. Parity plot comparing experimentally measured coverages of sec-alkylamines (C_3, C_4, and C_5) and the predicted coverages based on two adsorbate competitive Langmuir adsorption isotherm for C_3-C_4 (♦), and C_4-C_5 (●), fitted to a single relative adsorption enthalpy and entropy per mol CH_2 **B.** Adsorption enthalpy and entropy increment per mol CH_2 for alkanes (supporting information, **Sec. S8**) and alkylamines over H-ZSM-5 **C.** Alkylamine adsorbed on aluminosilicate Brønsted acid site, forming an alkylammonium ion, and alkane interaction with aluminosilicate Brønsted acid site upon adsorption.

Conclusion. While typically considered irreversible, alkylamine adsorption on aluminosilicate Brønsted acid sites was demonstrated to be reversible through adsorption-assisted desorption. Under conditions free of any significant transport limitations, the competitive adsorption of binary alkylamine mixtures allowed adsorption-desorption equilibria to be approached over H-ZSM-5 (Si/Al = 140), facilitating the measurement of the relative adsorption thermodynamics of alkylamines on mostly isolated Brønsted acid sites. Under reversible conditions, the fractional coverages of adsorbed alkylamines were quantitatively described by a Langmuir isotherm, from which standard-state adsorption enthalpy and entropy were extracted. Across the adsorption of 2-propan, 2-butan, and 2-pentanamine, each additional methylene unit (-CH_2-) provides a fixed enthalpic stabilization and entropic penalty. We propose that the enthalpy and entropy associated with methylene units results from electrostatic interactions between adsorbate alkyl chains and their surrounding pore environment, qualitatively similar to alkane adsorption in zeolites. While enthalpic information has previously been reported for adsorbed alkylamines,[13-16] and that free

energy is what influences the behavior of an adsorbate in a porous environment, the ability demonstrated here to measure adsorbate entropy will provide new information to aid in the design of functional porous materials.

Supporting Information. Details of the experimental setup, fractional coverage measurements, isotherm derivations, and FT-IR spectra are available in the supporting information.

Acknowledgements. The authors acknowledge financial support for this work from the National Science Foundation (Award Number CBET - 2045953).

References

(1) Farneth, W. E.; Gorte, R. J. Methods for Characterizing Zeolite Acidity. *Chemical Reviews* **1995**, *95* (3), 615-635. DOI: 10.1021/cr00035a007.
(2) Gorte, R. J. What do we know about the acidity of solid acids? *Catalysis Letters* **1999**, *62* (1), 1-13. DOI: 10.1023/A:1019010013989.
(3) Parrillo, D. J.; Adamo, A. T.; Kokotailo, G. T.; Gorte, R. J. Amine adsorption in H-ZSM-5. *Applied Catalysis* **1990**, *67* (1), 107-118. DOI: https://doi.org/10.1016/S0166-9834(00)84435-8.
(4) Abdelrahman, O. A.; Vinter, K. P.; Ren, L.; Xu, D.; Gorte, R. J.; Tsapatsis, M.; Dauenhauer, P. J. Simple quantification of zeolite acid site density by reactive gas chromatography. *Catalysis Science & Technology* **2017**, *7* (17), 3831-3841, 10.1039/C7CY01068K. DOI: 10.1039/C7CY01068K.
(5) Barzetti, T.; Selli, E.; Moscotti, D.; Forni, L. Pyridine and ammonia as probes for FTIR analysis of solid acid catalysts. *Journal of the Chemical Society, Faraday Transactions* **1996**, *92* (8), 1401-1407, 10.1039/FT9969201401. DOI: 10.1039/FT9969201401.
(6) Liu, D.; Zhang, X.; Bhan, A.; Tsapatsis, M. Activity and selectivity differences of external Brønsted acid sites of single-unit-cell thick and conventional MFI and MWW zeolites. *Microporous and Mesoporous Materials* **2014**, *200*, 287-290. DOI: https://doi.org/10.1016/j.micromeso.2014.06.029.
(7) Wu, Y.; Emdadi, L.; Qin, D.; Zhang, J.; Liu, D. Quantification of external surface and pore mouth acid sites in unit-cell thick pillared MFI and pillared MWW zeolites. *Microporous and Mesoporous Materials* **2017**, *241*, 43-51. DOI: https://doi.org/10.1016/j.micromeso.2016.12.004.
(8) Lawal, A.; Abdelrahman, O. A. Paired Site Characterization in Aluminosilicate Zeolites through Limited Alkylammonium Stability. *The Journal of Physical Chemistry C* **2023**, *127* (42), 20857-20869. DOI: 10.1021/acs.jpcc.3c04684.
(9) Pang, Y.; Ardagh, M. A.; Shetty, M.; Chatzidimitriou, A.; Kumar, G.; Vlaisavljevich, B.; Dauenhauer, P. J. On the Spatial Design of Co-Fed Amines for Selective Dehydration of Methyl Lactate to Acrylates. *ACS Catalysis* **2021**, *11* (9), 5718-5735. DOI: 10.1021/acscatal.1c00573.
(10) Murphy, B. M.; Letterio, M. P.; Xu, B. Selectivity Control in the Catalytic Dehydration of Methyl Lactate: The Effect of Pyridine. *ACS Catalysis* **2016**, *6* (8), 5117-5131. DOI: 10.1021/acscatal.6b00723.
(11) Chen, H.; Abdelrahman, O. A. Cooperative Adsorption: Solvating the Hofmann Elimination of Alkylamines. *ACS Catalysis* **2021**, *11* (11), 6416-6430. DOI: 10.1021/acscatal.1c01364.
(12) Gounder, R.; Iglesia, E. The Roles of Entropy and Enthalpy in Stabilizing Ion-Pairs at Transition States in Zeolite Acid Catalysis. *Accounts of Chemical Research* **2012**, *45* (2), 229-238. DOI: 10.1021/ar200138n.

(13) Lee, C.; Parrillo, D. J.; Gorte, R. J.; Farneth, W. E. Relationship between Differential Heats of Adsorption and Brønsted Acid Strengths of Acidic Zeolites: H-ZSM-5 and H-Mordenite. *Journal of the American Chemical Society* **1996**, *118* (13), 3262-3268. DOI: 10.1021/ja953452y.
(14) Patet, R. E.; Caratzoulas, S.; Vlachos, D. G. Adsorption in zeolites using mechanically embedded ONIOM clusters. *Physical Chemistry Chemical Physics* **2016**, *18* (37), 26094-26106, 10.1039/C6CP03266D. DOI: 10.1039/C6CP03266D.
(15) Lee, C. C.; Gorte, R. J.; Farneth, W. E. Calorimetric Study of Alcohol and Nitrile Adsorption Complexes in H-ZSM-5. *The Journal of Physical Chemistry B* **1997**, *101* (19), 3811-3817. DOI: 10.1021/jp970711s.
(16) Parrillo, D. J.; Gorte, R. J.; Farneth, W. E. A calorimetric study of simple bases in H-ZSM-5: a comparison with gas-phase and solution-phase acidities. *Journal of the American Chemical Society* **1993**, *115* (26), 12441-12445. DOI: 10.1021/ja00079a027.
(17) Campbell, C. T.; Sellers, J. R. V. The Entropies of Adsorbed Molecules. *Journal of the American Chemical Society* **2012**, *134* (43), 18109-18115. DOI: 10.1021/ja3080117.
(18) Dauenhauer, P. J.; Abdelrahman, O. A. A Universal Descriptor for the Entropy of Adsorbed Molecules in Confined Spaces. *ACS Central Science* **2018**, *4* (9), 1235-1243. DOI: 10.1021/acscentsci.8b00419.
(19) Gorte, R. J. Design parameters for temperature programmed desorption from porous catalysts. *Journal of Catalysis* **1982**, *75* (1), 164-174. DOI: https://doi.org/10.1016/0021-9517(82)90131-2.
(20) Tronconi, E.; Lietti, L.; Forzatti, P. Diffusion and readsorption effects during TPD from porous materials. *Thermochimica Acta* **1988**, *135*, 147-153. DOI: https://doi.org/10.1016/0040-6031(88)87379-9.
(21) Zhu, W.; van de Graaf, J. M.; van den Broeke, L. J. P.; Kapteijn, F.; Moulijn, J. A. TEOM: A Unique Technique for Measuring Adsorption Properties. Light Alkanes in Silicalite-1. *Industrial & Engineering Chemistry Research* **1998**, *37* (5), 1934-1942. DOI: 10.1021/ie970739q.
(22) Millot, B.; Methivier, A.; Jobic, H. Adsorption of n-Alkanes on Silicalite Crystals. A Temperature-Programmed Desorption Study. *The Journal of Physical Chemistry B* **1998**, *102* (17), 3210-3215. DOI: 10.1021/jp980090i.
(23) Rudzinski, W.; Panczyk, T. Kinetics of Gas Adsorption in Activated Carbons, Studied by Applying the Statistical Rate Theory of Interfacial Transport. *The Journal of Physical Chemistry B* **2001**, *105* (29), 6858-6866. DOI: 10.1021/jp004166y.
(24) Schmid, M.; Parkinson, G. S.; Diebold, U. Analysis of Temperature-Programmed Desorption via Equilibrium Thermodynamics. *ACS Physical Chemistry Au* **2023**, *3* (1), 44-62. DOI: 10.1021/acsphyschemau.2c00031.
(25) Parrillo, D. J.; Lee, C.; Gorte, R. J. Heats of adsorption for ammonia and pyridine in H-ZSM-5: evidence for identical Brønsted-acid sites. *Applied Catalysis A: General* **1994**, *110* (1), 67-74. DOI: https://doi.org/10.1016/0926-860X(94)80106-1.
(26) Kumar, G.; Ren, L.; Pang, Y.; Li, X.; Chen, H.; Gulbinski, J.; Dauenhauer, P. J.; Tsapatsis, M.; Abdelrahman, O. A. Acid Sites of Phosphorus-Modified Zeosils. *ACS Catalysis* **2021**, *11* (15), 9933-9948. DOI: 10.1021/acscatal.1c01588.
(27) Boudart, M. Adsorption assisted desorption in catalytic cycles. *Journal of Molecular Catalysis A: Chemical* **1999**, *141* (1), 1-7. DOI: https://doi.org/10.1016/S1381-1169(98)00244-1.

(28) Yamada, T.; Onishi, T.; Tamaru, K. Adsorption-desorption kinetics of carbon monoxide on palladium polycrystalline surfaces. *Surface Science* **1983**, *133* (2), 533-546. DOI: https://doi.org/10.1016/0039-6028(83)90018-3.
(29) Sobczyk, D. P.; Hesen, J. J. G.; van Grondelle, J.; Schuring, D.; de Jong, A. M.; van Santen, R. A. Adsorption Assisted Desorption of NH3 on γ-Alumina Studied with Positron Emission Profiling. *Catalysis Letters* **2004**, *94* (1), 37-43. DOI: 10.1023/B:CATL.0000019328.16620.1d.
(30) Gründling, C. H.; Eder-Mirth, G.; Lercher, J. A. Surface species in the direct amination of methanol over Brønsted acidic mordenite catalysts. *Research on Chemical Intermediates* **1997**, *23* (1), 25-40. DOI: 10.1163/156856797X00367.
(31) Ho, C. R.; Bettinson, L. A.; Choi, J.; Head-Gordon, M.; Bell, A. T. Zeolite-Catalyzed Isobutene Amination: Mechanism and Kinetics. *ACS Catalysis* **2019**, *9* (8), 7012-7022. DOI: 10.1021/acscatal.9b01799.
(32) Janda, A.; Bell, A. T. Effects of Si/Al Ratio on the Distribution of Framework Al and on the Rates of Alkane Monomolecular Cracking and Dehydrogenation in H-MFI. *Journal of the American Chemical Society* **2013**, *135* (51), 19193-19207. DOI: 10.1021/ja4081937.
(33) Abdelrahman, O.; Lawal, A. Paired Site Characterization in Aluminosilicate Zeolites through Limited Alkylammonium Stability. . *ChemRxiv. Cambridge: Cambridge Open Engage* **2023**, Journal. DOI: 10.26434/chemrxiv-2023-njh44-v2.
(34) Parrillo, D. J.; Gorte, R. J. Characterization of acidity in H-ZSM-5, H-ZSM-12, H-Mordenite, and H-Y using microcalorimetry. *The Journal of Physical Chemistry* **1993**, *97* (34), 8786-8792. DOI: 10.1021/j100136a023.
(35) Fang, H.; Zheng, A.; Xu, J.; Li, S.; Chu, Y.; Chen, L.; Deng, F. Theoretical Investigation of the Effects of the Zeolite Framework on the Stability of Carbenium Ions. *The Journal of Physical Chemistry C* **2011**, *115* (15), 7429-7439. DOI: 10.1021/jp1097316.
(36) Kazansky, V. B. Adsorbed carbocations as transition states in heterogeneous acid catalyzed transformations of hydrocarbons. *Catalysis Today* **1999**, *51* (3), 419-434. DOI: https://doi.org/10.1016/S0920-5861(99)00031-0.
(37) Yamadaya, S.; Oba, M.; Hasegawa, T.; Ogawa, K.; Kotera, Y. The mechanical strength of heterogeneous catalyst: I. The tensile strength of pelletized alumina catalysts. *Journal of Catalysis* **1970**, *19* (3), 264-270. DOI: https://doi.org/10.1016/0021-9517(70)90247-2.
(38) Grossman, S. It's A Matter of Degrees, but Do Degrees Really Matter? **2018**, Technical Literature Library. From Restek Restek Advantage.
(39) Maduskar, S.; Teixeira, A. R.; Paulsen, A. D.; Krumm, C.; Mountziaris, T. J.; Fan, W.; Dauenhauer, P. J. Quantitative carbon detector (QCD) for calibration-free, high-resolution characterization of complex mixtures. *Lab on a Chip* **2015**, *15* (2), 440-447, 10.1039/C4LC01180E. DOI: 10.1039/C4LC01180E.
(40) Kresnawahjuesa, O.; Gorte, R. J.; de Oliveira, D.; Lau, L. Y. A Simple, Inexpensive, and Reliable Method for Measuring Brønsted-Acid Site Densities in Solid Acids. *Catalysis Letters* **2002**, *82* (3), 155-160. DOI: 10.1023/A:1020514911456.
(41) Rudham, R.; Spiers, A. I.; Winstanley, A. W. The assessment of Brönsted acidity concentration in HY zeolites by propan-2-ol dehydration and other methods. *Zeolites* **1991**, *11* (8), 850-853. DOI: https://doi.org/10.1016/S0144-2449(05)80068-5.
(42) Corma, A.; Fornes, V.; Monton, J. B.; Orchilles, A. V. Catalytic cracking of alkanes on large pore, high SiO2/Al2O3 zeolites in the presence of basic nitrogen compounds. Influence of catalyst structure and composition in the activity and selectivity. *Industrial & Engineering Chemistry Research* **1987**, *26* (5), 882-886. DOI: 10.1021/ie00065a005.

(43) Caeiro, G.; Magnoux, P.; Ayrault, P.; Lopes, J. M.; Ribeiro, F. R. Deactivating effect of coke and basic nitrogen compounds during the methylcyclohexane transformation over H-MFI zeolite. *Chemical Engineering Journal* **2006**, *120* (1), 43-54. DOI: https://doi.org/10.1016/j.cej.2006.03.036.
(44) Choudhary, V. R.; Devadas, P.; Banerjee, S.; Kinage, A. K. Aromatization of dilute ethylene over Ga-modified ZSM-5 type zeolite catalysts. *Microporous and Mesoporous Materials* **2001**, *47* (2), 253-267. DOI: https://doi.org/10.1016/S1387-1811(01)00385-7.
(45) Hunter, K. C.; East, A. L. L. Properties of C−C Bonds in n-Alkanes: Relevance to Cracking Mechanisms. *The Journal of Physical Chemistry A* **2002**, *106* (7), 1346-1356. DOI: 10.1021/jp0129030.
(46) Hunter, E. P. L.; Lias, S. G. Evaluated Gas Phase Basicities and Proton Affinities of Molecules: An Update. *Journal of Physical and Chemical Reference Data* **1998**, *27* (3), 413-656. DOI: 10.1063/1.556018 (acccessed 6/15/2023).
(47) Savitz, S.; Myers, A. L.; Gorte, R. J.; White, D. Does the Cal-Ad Method Distinguish Differences in the Acid Sites of H-MFI? *Journal of the American Chemical Society* **1998**, *120* (23), 5701-5703. DOI: 10.1021/ja980157f.
(48) van Bokhoven, J. A.; Williams, B. A.; Ji, W.; Koningsberger, D. C.; Kung, H. H.; Miller, J. T. Observation of a compensation relation for monomolecular alkane cracking by zeolites: the dominant role of reactant sorption. *Journal of Catalysis* **2004**, *224* (1), 50-59. DOI: https://doi.org/10.1016/j.jcat.2004.02.003.
(49) Eder, F.; Lercher, J. A. Alkane sorption in molecular sieves: The contribution of ordering, intermolecular interactions, and sorption on Brønsted acid sites. *Zeolites* **1997**, *18* (1), 75-81. DOI: https://doi.org/10.1016/S0144-2449(96)00127-3.
(50) Savitz, S.; Siperstein, F.; Gorte, R. J.; Myers, A. L. Calorimetric Study of Adsorption of Alkanes in High-Silica Zeolites. *The Journal of Physical Chemistry B* **1998**, *102* (35), 6865-6872. DOI: 10.1021/jp981836f.
(51) Denayer, J. F.; Souverijns, W.; Jacobs, P. A.; Martens, J. A.; Baron, G. V. High-Temperature Low-Pressure Adsorption of Branched C5−C8 Alkanes on Zeolite Beta, ZSM-5, ZSM-22, Zeolite Y, and Mordenite. *The Journal of Physical Chemistry B* **1998**, *102* (23), 4588-4597. DOI: 10.1021/jp980674k.
(52) Arik, I. C.; Denayer, J. F.; Baron, G. V. High-temperature adsorption of n-alkanes on ZSM-5 zeolites: influence of the Si/Al ratio and the synthesis method on the low-coverage adsorption properties. *Microporous and Mesoporous Materials* **2003**, *60* (1), 111-124. DOI: https://doi.org/10.1016/S1387-1811(03)00332-9.
(53) De Moor, B. A.; Reyniers, M.-F.; Gobin, O. C.; Lercher, J. A.; Marin, G. B. Adsorption of C2−C8 n-Alkanes in Zeolites. *The Journal of Physical Chemistry C* **2011**, *115* (4), 1204-1219. DOI: 10.1021/jp106536m.
(54) Eder, F.; Stockenhuber, M.; Lercher, J. A. Brønsted Acid Site and Pore Controlled Siting of Alkane Sorption in Acidic Molecular Sieves. *The Journal of Physical Chemistry B* **1997**, *101* (27), 5414-5419. DOI: 10.1021/jp9706487.
(55) Eder, F.; Lercher, J. A. On the Role of the Pore Size and Tortuosity for Sorption of Alkanes in Molecular Sieves. *The Journal of Physical Chemistry B* **1997**, *101* (8), 1273-1278. DOI: 10.1021/jp961816i.
(56) Yeh, Y.-H.; Gorte, R. J.; Rangarajan, S.; Mavrikakis, M. Adsorption of Small Alkanes on ZSM-5 Zeolites: Influence of Brønsted Sites. *The Journal of Physical Chemistry C* **2016**, *120* (22), 12132-12138. DOI: 10.1021/acs.jpcc.6b03855.

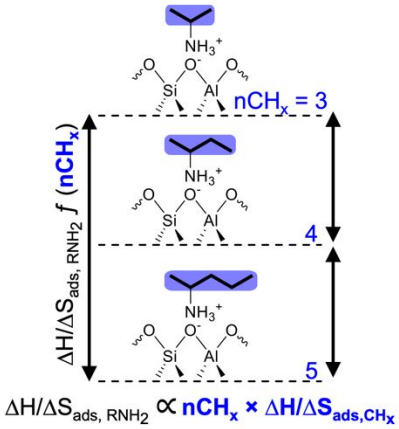
NH3+
O
O-
O
Si
Al
nCHx = 3
4
5
ΔH/ΔSads, RNH2 f (nCHx)
ΔH/ΔSads, RNH2 ∝ nCHx × ΔH/ΔSads,CHx

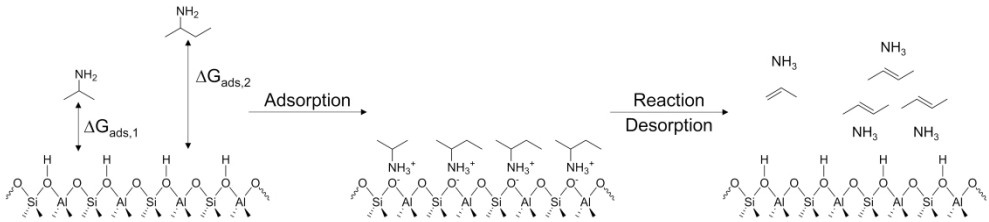

Scheme 1. Competitive adsorption between 2-propanamine and 2-butanamine over Brønsted acid sites, where relative coverages at equilibrium are dictated by relative free energies of adsorption. Coverages of the different alkylamines on the surface can be directly measured by quantifying their respective Hofmann elimination alkene product.

203x46mm (600 x 600 DPI)

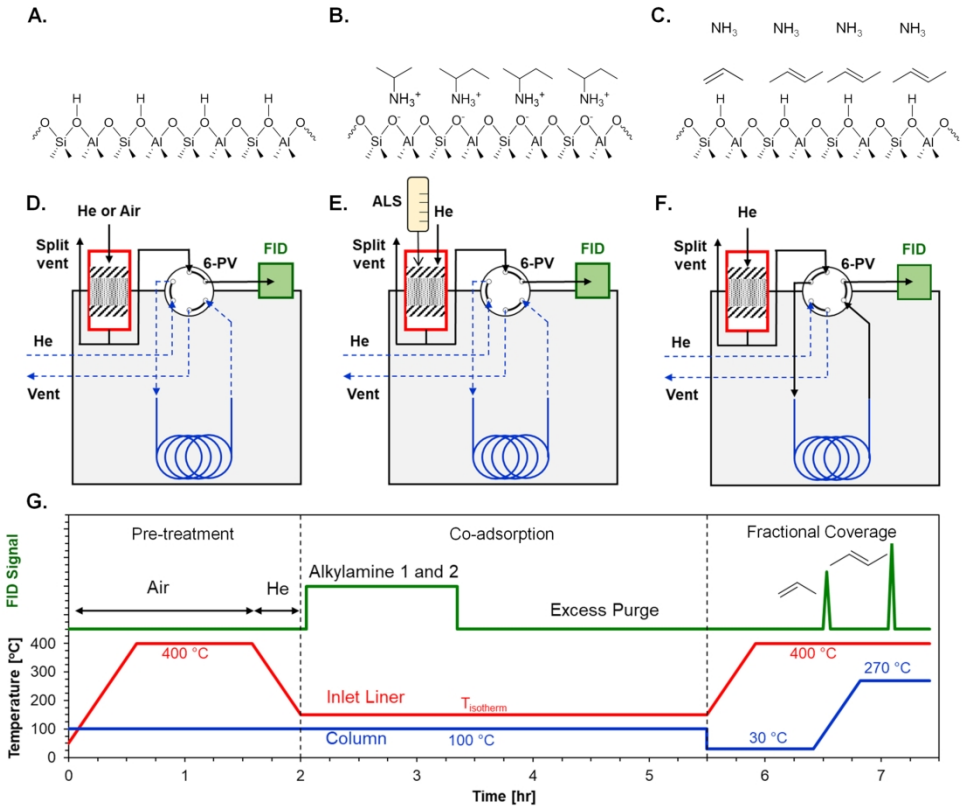

Figure 1. Reactive Gas Chromatography (RGC) to measure co-adsorbed alkylamine coverage A. Aluminosilicate Brønsted acid sites **B.** 2-propanamine and 2-butanamine adsorption on Brønsted acid sites, fractional coverages are determined by relative adsorption energetics and partial pressures **C.** Reactive desorption via Hofmann elimination, forming propene, butene(s) and ammonia **D. Pre-treatment:** Zeolite calcined in-situ at 673 K, cooled to co-adsorption temperature under helium atmosphere **E. Co-adsorption:** An automatic liquid sampler (ALS) injects a pre-determined mixture of alkylamines into a helium flow, creating a relative alkylamine partial pressure ($P_{Alkylamine,1}/P_{Alkylamine,2}$) that co-adsorbs on the zeolite surface, then purged to remove physisorbed amines **F. Fractional Coverage:** Linear temperature ramp of zeolite to 673 K while desorbing alkenes are trapped in chromatography column held at 303 K. The column temperature is linearly ramped to elute trapped alkenes corresponding to alkylamines adsorbed on Brønsted acid sites, independently quantified via a flame ionization detector (FID) **G. Temporal Profile:** Zeolite containing quartz liner temperature, chromatography column temperature, and corresponding FID signal as a function of time during pre-treatment, alkylamine co-adsorption, and fractional coverage estimation.

203x168mm (300 x 300 DPI)

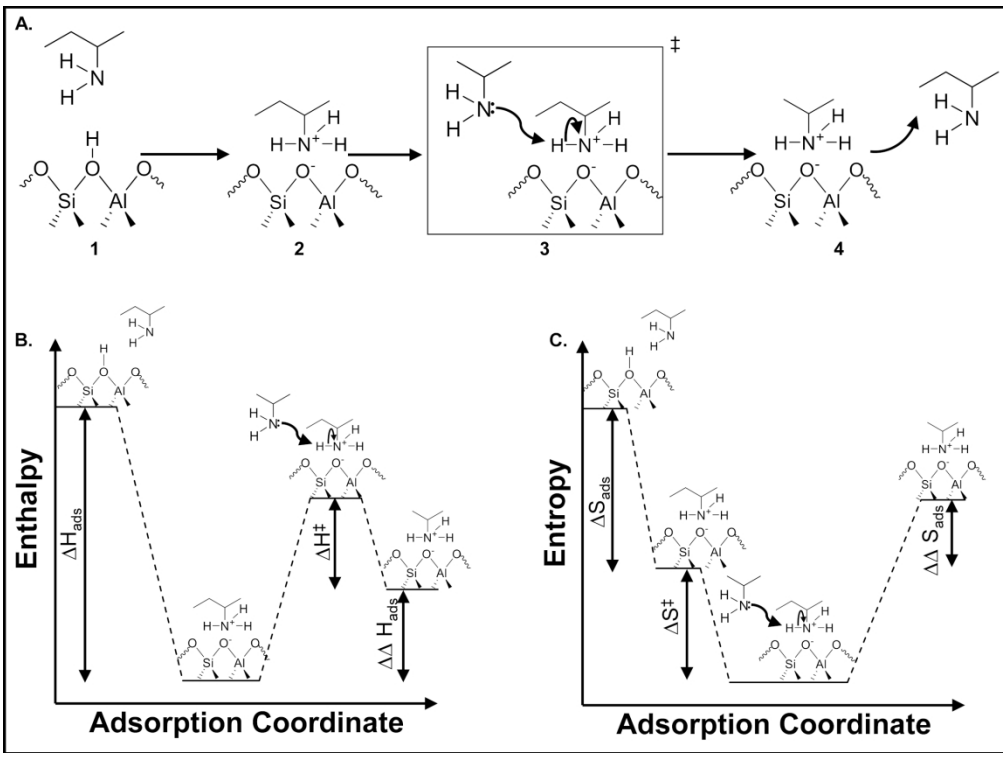

Scheme 2. Alkylamine Adsorption-Assisted Desorption over an Aluminosilicate Brønsted Acid Site
A. Adsorption of 2-butanamine onto an aluminosilicate Brønsted acid site, followed by a proton abstraction and its subsequent desorption by 2-propanamine **B.** Adsorption enthalpy of 2-propanamine and the relative adsorption enthalpy of 2-butanamine as it is displaced by 2-propanamine from the surface through an activated complex of both amines **C.** Adsorption entropy of 2-propanamine and the relative adsorption entropy of 2-butanamine as it is displaced by 2-propanamine from the surface, while forming an activated complex of both amines.

101x75mm (600 x 600 DPI)

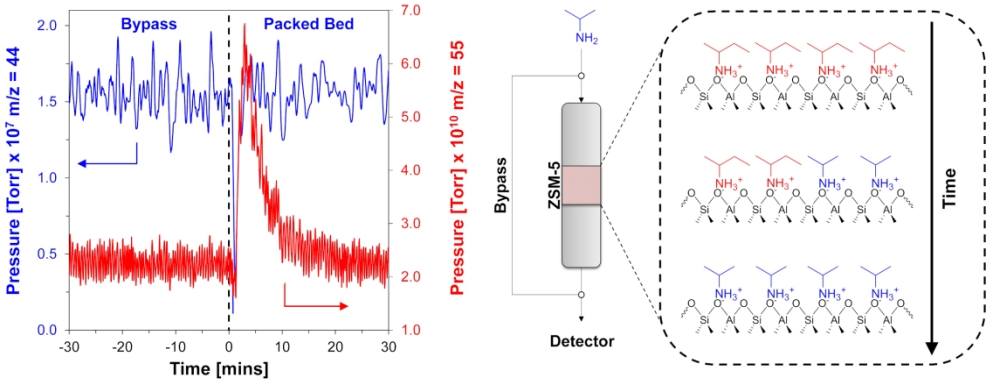

Figure 2. 2-propanamine-Assisted Desorption of 2-butanamine on H-ZSM-5. Breakthrough of 2-propanamine adsorption-assisted desorption over a 2-butylammonium saturated H-ZSM-5 at 423 K. Effluent 2-propanamine and 2-butanamine were tracked through mass to charge ratios (m/z) of 44 and 55, respectively.

101x38mm (600 x 600 DPI)

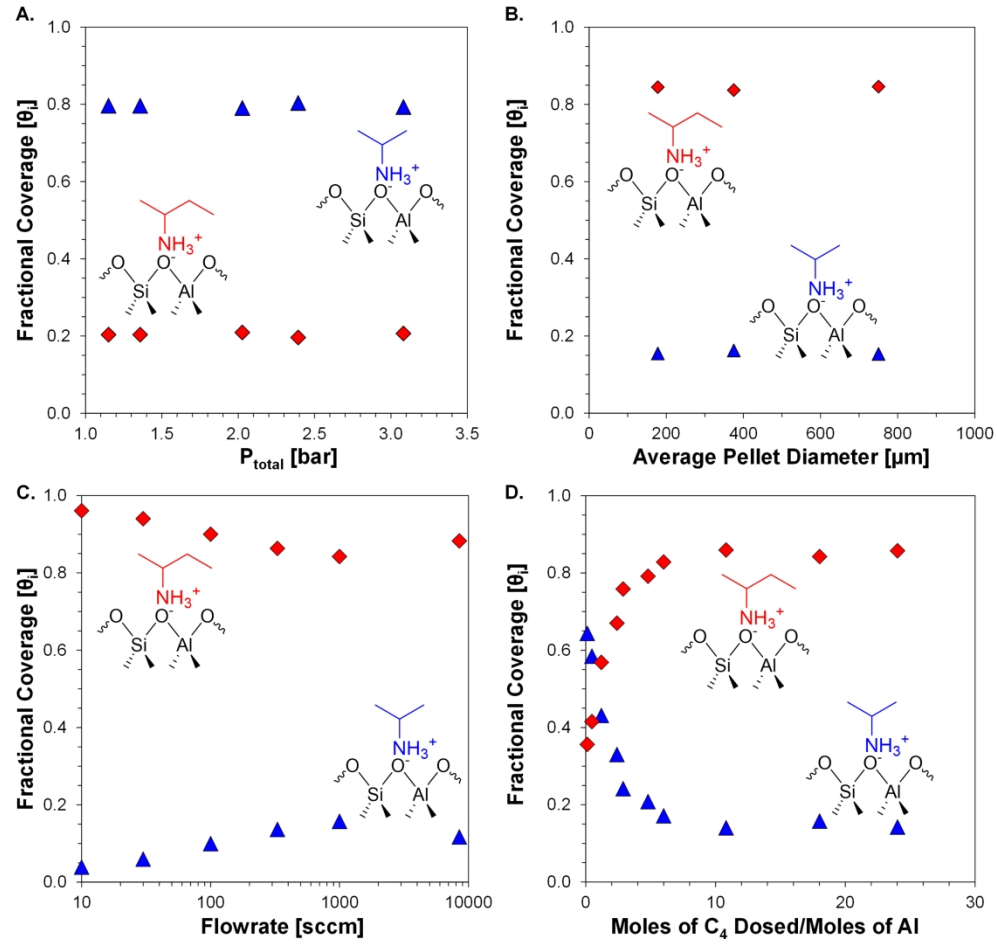

Figure 3. Fractional coverage of C3 (▵), and C4 (♦) on H-ZSM-5 at 423 K as a function of A. Total pressure, P_{C3}/P_{C4} = 50 **B.** Average zeolite pellet diameter, P_{C3}/P_{C4} = 3 **C.** He carrier gas flow rate, P_{C3}/P_{C4} = 3 **D.** Alkylamine extent of exposure (Eq. 6), P_{C3}/P_{C4} = 3.

203x191mm (600 x 600 DPI)

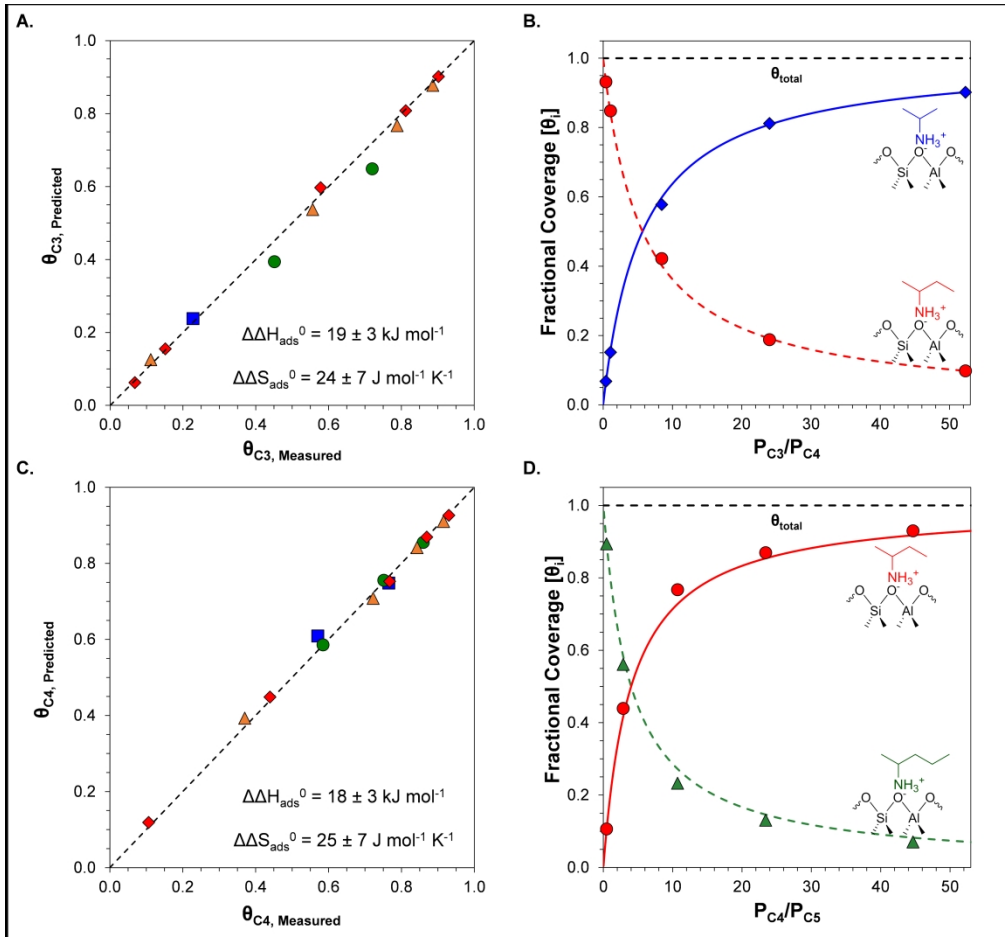

Figure 4. Alkylamine co-adsorption over H-ZSM-5 A. Parity plot comparing measured and predicted coverages of C_3 at 373 (■), 423 (●), 473 (△) and 498 K (♦), based on a two-adsorbate competitive Langmuir adsorption isotherm for C_3 and C_4. **B.** Fractional coverages of C_3 (♦) and C_4 (●) as a function of their relative partial pressure at 498 K, θtotal indicates the total coverage **C.** Parity plot comparing measured and predicted coverages of C_4 at 373 (■), 423 (●), 473 (△) and 498 K (♦), based on a two-adsorbate competitive Langmuir adsorption isotherm for C_4 and C_5 D. Fractional coverages of C_4 (●) and C_5 (△) as a function of their relative partial pressure at 498 K, θ_{total} indicates the total coverage.

217x203mm (600 x 600 DPI)

A.

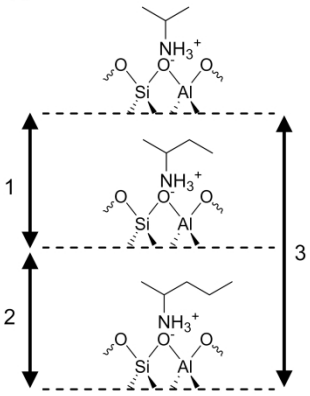

B.

			$\Delta\Delta H_{ads}$ [kJ mol^{-1}]	$\Delta\Delta S_{ads}$ [J mol^{-1} K^{-1}]
1	C_3-C_4	Measured	19 ± 3	24 ± 7
2	C_4-C_5	Measured	18 ± 3	25 ± 7
3	C_3-C_5	Predicted (1+2)	37	49
	C_3-C_5	Measured	36 ± 22	56 ± 29

C.

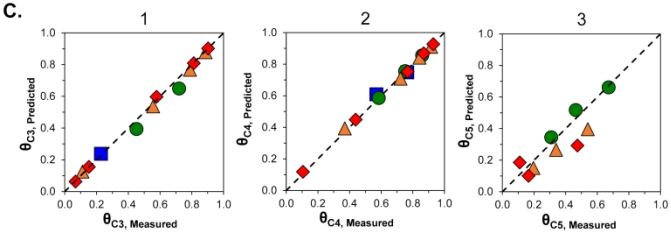

Figure 5. Relative adsorption energetics of C_3, C_4, and C_5 A. Relative energy levels of adsorbed 2-propylammonium (C_3), 2-butylammonium (C_4), and 2-pentylammonium (C_5). C_3-C_4 (1), C_4-C_5 (2), and C_3-C_5 (3) **B.** Comparison of measured and predicted C_3-C_5 relative adsorption enthalpy and entropy, per Eqs. 9-10 **C.** Parity plot comparing measured and predicted coverages at 373 (■), 423 (●), 473 (△) and 498 K (♦) based on two-adsorbate competitive Langmuir adsorption isotherms of C_3-C_4 (1), C_4-C_5 (2), and C_3-C_5 (3).

203x94mm (600 x 600 DPI)

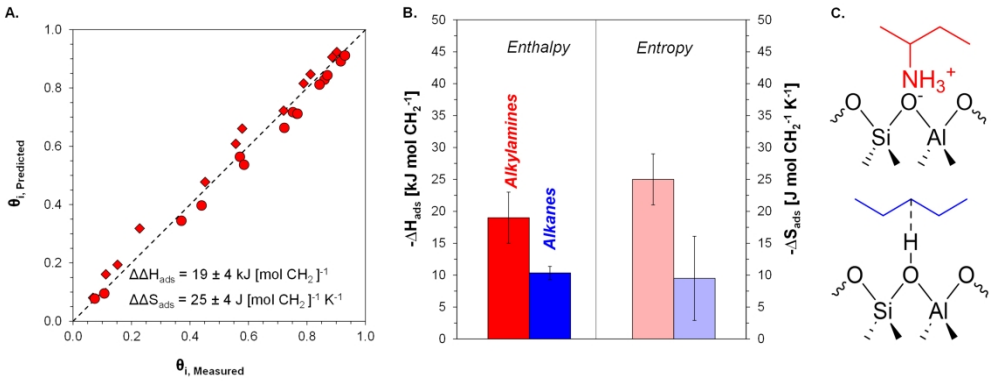

Figure 6. Adsorption Energetics per Methylene Unit of Alkanes and Alkylamines. A. Parity plot comparing experimentally measured coverages of sec-alkylamines (C_3, C_4, and C_5) and the predicted coverages based on two adsorbate competitive Langmuir adsorption isotherm for C_3-C_4 (♦), and C_4-C_5 (●), fitted to a single relative adsorption enthalpy and entropy per mol CH_2 **B.** Adsorption enthalpy and entropy increment per mol CH_2 for alkanes (supporting information, Sec. S8) and alkylamines over H-ZSM-5 **C.** Alkylamine adsorbed on aluminosilicate Brønsted acid site, forming an alkylammonium ion, and alkane interaction with aluminosilicate Brønsted acid site upon adsorption.

203x77mm (600 x 600 DPI)